

Micro-discharge Micro-thruster

John Slough*, Samuel Andreason, Timothy Ziemba
University of Washington, Seattle, WA, 98195

J.J Ewing
Ewing Technology Associates, Bellevue, WA, 98006

This paper summarizes the experiments and analysis of the micro-discharge micro-thruster developed jointly by Ewing Technology Associates and the University of Washington. The key experimental result has been the demonstration of a sustained discharge in a very simple micro-discharge type of structure (aperture ~ 300 micron) under demanding flow conditions. The micro-discharge provides for power addition to the neutral gas in discharges that transition from relatively high pressure (~ 10 - 30 Torr) to vacuum on the supersonic flow side of the limiting aperture “nozzle” separating the discharge region from the vacuum region. The fact that a fairly stable discharge is maintained on the downstream side suggests that the fairly hot plasma (~ 2 eV) deposits power into the neutral gas (Argon) in a manner that produces a neutral flow of similar energy, much like an arcjet but at very low power (1-5 W). A crude measurement of the power deposition into the gas via an energy balance approach was obtained from thermocouple measurements, which also imply that the gas temperature may be as high as 1-2 eV. Thrust measurements as well as characterization of discharge and plasma properties are an integral part of the current experimental work. Concurrently, a numerical model is being developed to explain the gas and plasma dynamics involved in the device. A description of the device, the experimental setup as well as results from the experiments will be presented.

Nomenclature

i	=	time index
P	=	pressure in Pa
T	=	temperature in eV

I. Introduction

WITH the current development of ever smaller spacecraft, there will be a parallel need for micropropulsion devices that are not only very low mass but can also operate at very low power. In response to this need work on a wide array of devices has taken place¹⁻³. Future nano-spacecraft (nanosats) will require significant propulsion capability in order to provide a high degree of maneuverability and capability. Given the likely presence of onboard electrical power generation, there would be significant benefit from using electric propulsion (EP) for improving the efficiency of propellant use as well as an increase in exhaust velocity (Isp). The leveraged use of spacecraft assets in this way adds to the simplicity of operation and reduction of spacecraft mass. Current efforts under development are targeted for spacecraft mass ~100 kg with an available power level for propulsion of ~ 100 watts. There are several propulsion systems, initially developed for much higher powers, that are now being redesigned for this lower power regime. In this group, significant development has been put into low power versions of ion thrusters, Hall thrusters, and the PPT⁴. There are also novel devices that work primarily at low power such as field emission thrusters, vaporizing liquid thrusters, resistojets, microwave arcjets, and micro-arcjets⁵.

*AIAA member

Report Documentation Page			Form Approved OMB No. 0704-0188		
Public reporting burden for the collection of information is estimated to average 1 hour per response, including the time for reviewing instructions, searching existing data sources, gathering and maintaining the data needed, and completing and reviewing the collection of information. Send comments regarding this burden estimate or any other aspect of this collection of information, including suggestions for reducing this burden, to Washington Headquarters Services, Directorate for Information Operations and Reports, 1215 Jefferson Davis Highway, Suite 1204, Arlington VA 22202-4302. Respondents should be aware that notwithstanding any other provision of law, no person shall be subject to a penalty for failing to comply with a collection of information if it does not display a currently valid OMB control number.					
1. REPORT DATE JUN 2005		2. REPORT TYPE		3. DATES COVERED -	
4. TITLE AND SUBTITLE Micro-discharge Micro-thruster			5a. CONTRACT NUMBER FA8650-04-C-2514		
			5b. GRANT NUMBER		
			5c. PROGRAM ELEMENT NUMBER		
6. AUTHOR(S) John Slough; Samuel Andreason; Timothy Ziemba; J Ewing			5d. PROJECT NUMBER OSDB		
			5e. TASK NUMBER R4QL		
			5f. WORK UNIT NUMBER		
7. PERFORMING ORGANIZATION NAME(S) AND ADDRESS(ES) Ewing Technology Associates,Bellevue,WA,98006			8. PERFORMING ORGANIZATION REPORT NUMBER		
9. SPONSORING/MONITORING AGENCY NAME(S) AND ADDRESS(ES)			10. SPONSOR/MONITOR'S ACRONYM(S)		
			11. SPONSOR/MONITOR'S REPORT NUMBER(S)		
12. DISTRIBUTION/AVAILABILITY STATEMENT Approved for public release; distribution unlimited					
13. SUPPLEMENTARY NOTES					
14. ABSTRACT This paper summarizes the experiments and analysis of the micro-discharge microthruster developed jointly by Ewing Technology Associates and the University of Washington. The key experimental result has been the demonstration of a sustained discharge in a very simple micro-discharge type of structure (aperture ~ 300 micron) under demanding flow conditions. The micro-discharge provides for power addition to the neutral gas in discharges that transition from relatively high pressure (~ 10 - 30 Torr) to vacuum on the supersonic flow side of the limiting aperture "nozzle" separating the discharge region from the vacuum region. The fact that a fairly stable discharge is maintained on the downstream side suggests that the fairly hot plasma (~ 2 eV) deposits power into the neutral gas (Argon) in a manner that produces a neutral flow of similar energy, much like an arcjet but at very low power (1-5 W). A crude measurement of the power deposition into the gas via an energy balance approach was obtained from thermocouple measurements, which also imply that the gas temperature may be as high as 1-2 eV. Thrust measurements as well as characterization of discharge and plasma properties are an integral part of the current experimental work. Concurrently, a numerical a model is being developed to explain the gas and plasma dynamics involved in the device. A description of the device, the experimental setup as well as results from the experiments will be presented.					
15. SUBJECT TERMS					
16. SECURITY CLASSIFICATION OF:			17. LIMITATION OF ABSTRACT	18. NUMBER OF PAGES 8	19a. NAME OF RESPONSIBLE PERSON
a. REPORT unclassified	b. ABSTRACT unclassified	c. THIS PAGE unclassified			

While these devices may have applicability at the 100 watt level, there have been only limited investigations of EP thrusters that operate at 10 watts and below. By necessity a nanosat thruster must be simple and require very little power processing and related hardware. A cold gas thruster fed by a micro valve and propellant tank is an example of the kind of simplicity that is desired⁶. Assuming that a thruster of this type is already available onboard the nanosat, it would be advantageous to add additional capability to this device with the addition of the available onboard power which would most likely be in the range of 1 to 10W at low voltage. A simple first choice would be to add energy to the gas via a DC discharge. It has been demonstrated that a very low power DC arcjet can provide for a fairly efficient thruster (up to 40%) in the 10 to 40 watt range at an Isp of 200 to 300s⁷. The structural simplicity of an arcjet may be favorable for both size and mass reduction of the conventional thruster; but there are difficulties in size reduction of the arcjet to the sub-centimeter scale. The simplest geometry that one can imagine for a micro-thruster in the context of a very low power DC discharge is that shown in Figure 1. In this scheme one has two electrodes separated by an insulator with a small hole bored through. The insulator acts as a discharge gap as well as nozzle in this configuration. The objective of this study is to investigate the fundamental discharge characteristics and performance of this type of very low power DC discharge.

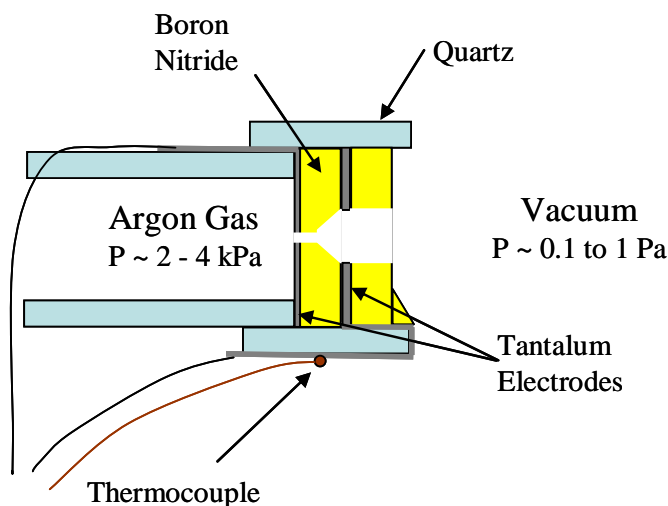


Figure 1. Schematic of a basic DC micro-discharge in a thruster configuration. Entry orifice in upstream electrode was 300 μm in diameter. Exit orifice and electrode varied from 300 μm to 2.5 mm . electrode separation was fixed at 1.5 mm.

Specifically, the aim was to study the discharge in a range of electrical input power from approximately 1 to 5 watts, and in a configuration suitable for generating thrust in a vacuum. The next step in development will be to determine which of the possible electrode configurations studied provides for the best performance in terms of thrust, Isp, and efficiency by measurements on a suitable thrust stand. The first goal however must be to determine what are the relevant conditions (sizes, shapes, voltages, materials) required for an appropriate microdischarge in a thruster configuration, where it must be kept in mind that simplicity and longevity need to be primary attributes of the final thruster configuration.

II. Experimental Setup

Several different configurations of the microdischarge are possible, and in fact several were fabricated and tested. From the early testing it was clear that the most successful electrode and insulator arrangements had several elements in common: By having a discharge in such a small geometry, even though the power was quite low, the power density in the propellant can be as high as several MW/kg. It quickly became clear that the electrode and insulating material needed to be made from suitable high temperature materials. All electrodes were thus constructed from tantalum (Ta) foil 0.13 mm thick. This material was chosen as it has the lowest sputtering yield of all metals from ion impact in the several hundred eV range. Tantalum also has a high thermal conductivity (57.5 W/m-°K) and melting point (3270 °K). It is similar to Molybdenum and Tungsten in first ionization potential (7.9 eV) and electron work function (4.25 eV), but is far more ductile, and was easily drilled and fashioned at small dimension. The electrode insulators were constructed from Boron Nitride (BN). It too has excellent thermal properties, and can easily be machined at small scale. The thruster was assembled with the electrodes and insulators mounted in either a BN or quartz (fused silica) tube with an inner bore of 6.4 mm (see Fig.1). The thruster was attached to the end of a 6.35 mm (1/4") quartz or alumina tube, 30 cm in length, with a high temperature, non-conducting alumina based cement. This secured the thruster as well as provided a sealed path for the conduction of the gas (Argon) propellant. The upstream Ta electrode was fashioned with a pigtail that passed between the quartz tube and thruster housing to where it was crimped to insulated magnet wire. A similar procedure was used for the exit electrode. The two wires were conducted from the vacuum chamber via an insulated feed thru. The wires were secured and all exposed metal

was insulated using 0.1mm thick Kapton® tape. The thruster was thus electrically and thermally isolated from the vacuum chamber. A thermocouple was occasionally mounted to the thruster body wall to measure heat flow to the thruster from the discharge, as well as obtain the equilibrium thruster body temperature. The thermocouple leads were insulated and routed out through an isolated feed thru as well.

The vacuum chamber was essentially composed of a 15 cm diameter cross with the thruster positioned at the center from a side port (see Fig.2). This allowed for both end-on viewing access as well as several side ports for diagnostic access. The system was pumped by a 360 l/s turbo-molecular pump. The system base pressure was 13 μPa (1×10^{-7} Torr). While the thruster was operating, the background pressure ranged from 0.1 to 1 Pa. The gas flow to the thruster was regulated by a mass flow controller, and the chamber pressure was measured with a capacitive monometer and cold cathode gauge.

The principle diagnostics of the discharge were voltage and current monitors and a 4 channel, 200 MHz digital oscilloscope that was battery powered and floated during thruster measurements. The discharge current was obtained by a 1 k Ω sense resistor in series with the discharge leads. All measurements were made by electrically isolated meters. A wide bandwidth spectrometer (350 nm to 850 nm) was used to characterize the plasma plume and internal discharge visible emissions. A calibrated photodiode was used to estimate radiated power loss. Pictures of the thruster in operation, as well as before and after extended periods of operation were obtained with a digital SLR camera. Detailed images of the thruster alignment and erosion were obtained from a stereoscopic microscope.

Two different power supplies were employed in the operation of the discharge. A 1500V DC, 10 mA supply with isolated output was used initially. It was found that there was a significant capacitance to ground from either lead (~ 100 nF). As small as this is, it had a profound effect on the discharge (see next section). A more space

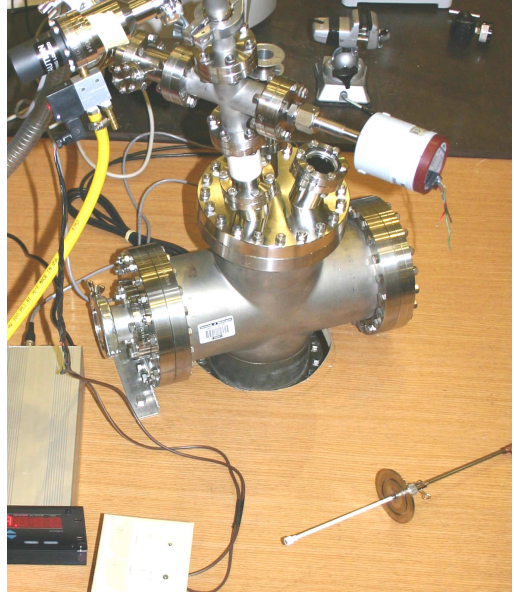


Figure 2. Picture of Vacuum chamber and test micro-thruster.

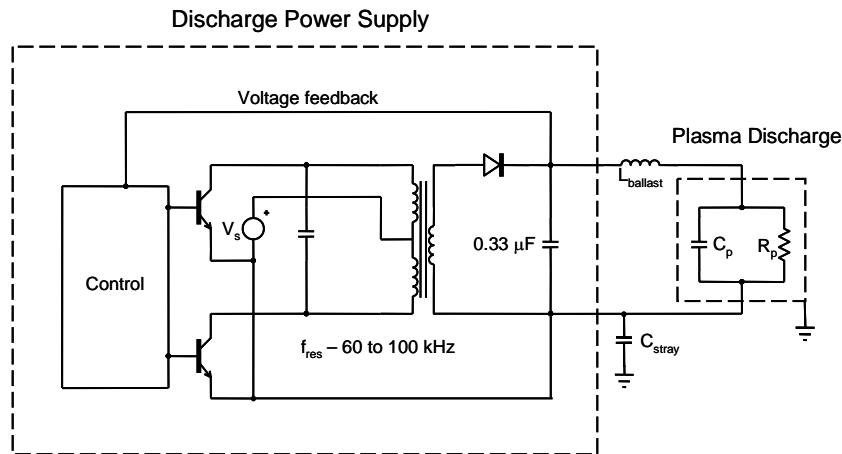


Figure 3. Circuit diagram of micro-discharge and power supply. The microdischarge capacitance $C_p = 50$ pF was primarily from the lead wires. The ballast inductor $L_{ballast} = 0.28$ H. The discharge resistance ranged from 50k Ω to 400 k Ω . The stray capacitance of the driver circuit to ground ~ 1 pF when battery powered and 100 pF when AC powered via transformer-rectifier.

sustainment at several mA was 60 k Ω . With the inductive ballast, it was possible to operate with only the 250 Ω of

relevant power supply was constructed that was capable of producing 950 V DC and 6 mA from six 1.5 V D cell batteries. A simplified circuit for the device with plasma load is given in Fig.3. This power supply had negligible AC ripple ($< 0.01\%$). The design is derived from the type of circuit used to power cold cathode fluorescent lamps and is very stable and efficient. Due to the inherent oscillatory nature of the self resonating transformer charging circuit ($f_{res} \sim 70$ kHz), it was possible to make use of a large value choke (~ 0.3 H) as a ballast rather than a resistor commonly used to produce a stable discharge of this kind. When a resistive ballast was used, a typical value for the resistor needed for discharge initiation and

resistance derived from the small choke windings. Without the need for a ballast resistor, the power processing unit ran with near unit efficiency.

III. Experimental Results

In this study, the conditions for stable operation and flow of a plasma in a discharge exposed to vacuum were conducted. From measurements of heat flow in the thruster a sense of both thrust and efficiency was obtained. Due to the extremely small power flow in the system it was not possible to use the usual plasma diagnostics in obtaining information. The diagnostics that were employed focused at measurement of parameters that could be measured with minimal disturbance of the discharge system. It was discovered that it was very difficult to perform the discharge experiments without influence from the external environment. Isolation of the microdischarge and power supply was critical. Ultimately one can not eliminate but only diminish the coupling to the vacuum chamber and supply, as there is always some capacitive coupling to the external driver circuit. The plasma flow itself connects electrically the discharge to the vacuum vessel wall and hence the system ground. Charge neutrality for the plasma is eventually enforced at this boundary. While it is believed that only a small fraction of the jet power is represented in the flow of charged particles (plasma), it is the medium through which the neutral gas is heated, and its behavior will determine where the heating occurs and what part of the thruster receives the greatest power flow and erosion. It was found that a wide range in discharge behavior was observed that correlated with subtle or minor changes in the discharge circuit. After some effort, a driver circuit was designed that minimized the stray coupling between the discharge circuit and chamber. There is still the artificiality of the vacuum boundary that would not be present in the same way in space, but limited testing in a much larger chamber (volume $\sim 8 \text{ m}^3$) at vacuum indicated that the results of the testing in the smaller chamber were at least qualitatively the same. Further testing is planned in both this large chamber and a large dielectric chamber to quantify chamber influence on the discharge and thruster characteristics in a much more space-like environment.

The reason for the particular sensitivity of this thruster to environmental influence stems from the very small power required to sustain the discharge. A small current flow due to stray capacitive coupling is a minor effect in most thrusters even in the 100 Watt class. For a micro-discharge, even a stray coupling capacitance 50 pF observed for the power leads provides for a power flow of several watts at a frequency of 30 kHz (an oscillation frequency commonly observed in the discharge current and voltage). Larger coupling to the chamber was observed to fundamentally modify the discharge to the point of modulating the discharge off and on at the characteristic frequency.

A grounding of the discharge supply resulted in major changes in the discharge. The most significant change in the discharge was observed with the electrode orientation having the exit electrode as the anode, the same as it is in an arcjet. A plasma plume was only observed when there was a DC ground connection of the power supply. When the discharge was isolated as shown in Fig. 3, the discharge was observed to be most intense in the channel with the plume protruding into the upstream gas plenum (see Fig.4). This discharge operated in the same flow regime as the case with the exit electrode as the cathode. It typically operated with a lower sustainment voltage for the same discharge current (was less resistive). The complete absence of plasma in the vacuum however should not be inferred that this configuration would not be effective as a thruster. The neutral flow from the exit nozzle is the same as the cathode exit electrode, and there was still an intense discharge maintained in the thruster throat. The thruster heating rate and final temperature was similar for both polarities indicating roughly the same heating and thus thruster efficiency.

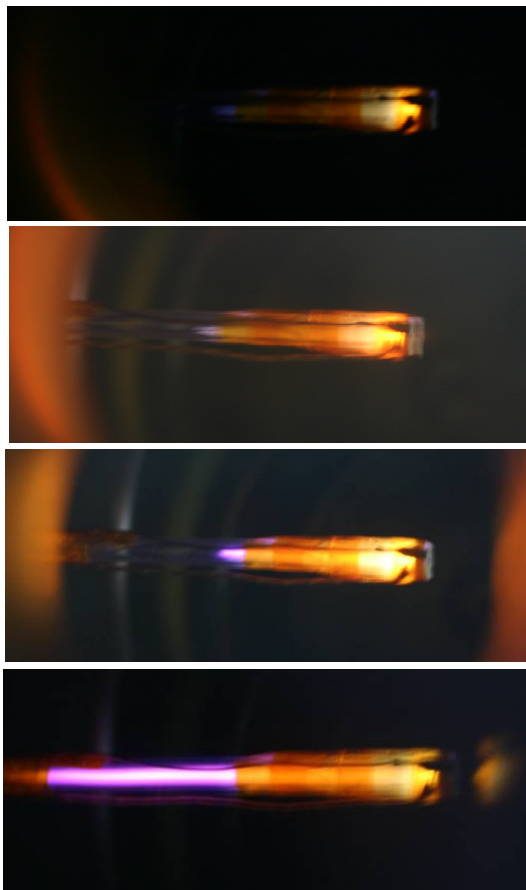


Figure 4. Micro-discharge with exit anode. *The sequence from top to bottom reflects a reduction in upstream pressure from 20 to 5 Torr Argon.*

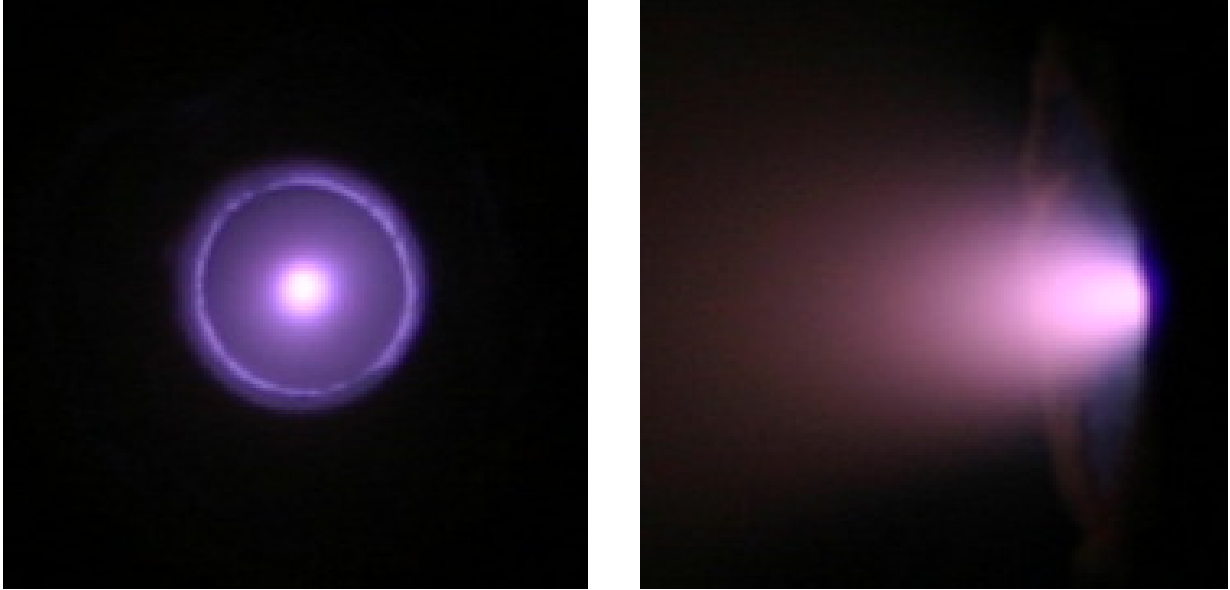


Figure 5. End-on and side-on pictures of the microdischarge microthuster with the exit electrode as cathode. The discharge geometry is that of Figure 1. The aperture for both of these pictures was 5.6. The time exposure was $1/100^{\text{th}}$ s for the end-on and a factor of 10 longer for side-on exposure.

Only measurement on a thrust stand will determine which mode is superior. Cathode erosion was observed for both modes of discharge operation, but longevity tests have not been performed to the extent that would determine which configuration is superior in this respect. With the suspicion that having the discharge plume occur back into the gas plenum was not an optimum condition, most of the discharge characterization was done with the cathode as the exit electrode producing a plasma plume into the vacuum region. A frontal and side-on picture of the discharge is shown in Fig.5. The discharge intensity was clearly greatest in the small bore ($300\ \mu\text{m}$) channel between electrodes under all operating conditions. An estimation of the light emission was made based on a photodiode and the observed

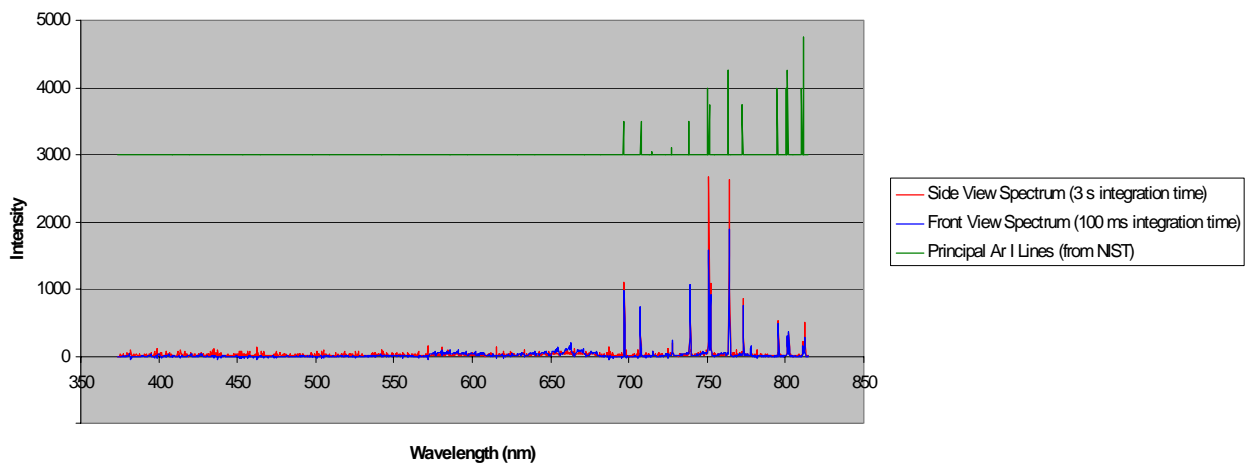


Figure 6. Visible spectrum from micro-discharge channel and plume The NIST compilation of lines for Ar matches well with the observed emission though the intensities are modified by electron temperature effects. Front view is primarily light from discharge channel. The side view spectrum monitored only plume emission. Integration times reflect difference in emission intensity.

emission spectrum (shown in Fig.6). These measurements indicate roughly 2 mW of line radiation loss. From the relative line ratios from a subset of neutral Ar I lines, an electron temperature between 1.5 and 2 eV is inferred. This assumes LTE which may not be strictly valid at the lower neutral and ion densities, but is what one would expect from ionization requirements. There was a significant difference in the spectra from the configuration where the cathode was the exit electrode. There was detectable emission in the blue from several Ar II ion lines. The neutral line ratios did not indicate a hotter electron population, so that it is likely that significant recombination occurs for the upstream cathode and plume.

The micro-discharge could be sustained for mass flow rates ranging from 0.25 to 4 mg/s. At the lower limit, the internal pressure in the thruster channel was not sufficient for breakdown at the maximum applied voltage (900 V) in Argon. The back side of the Paschen curve for Ar occurs at a pressure-length (P-d) product of less than 200 Pa-mm, indicating mean channel pressure of a few hundred to 1 kPa for discharge initiation and sustainment. At the upper mass flow rate the P-d product in the background chamber from the thruster to the wall approaches the Paschen minimum and spontaneous discharge to the wall from both the thruster and wire leads was sporadically observed. Given the isolation of the thruster and supply, this discharge was produced primarily through capacitive coupling. The optimum range of operation for the electrode geometry shown in Fig.1 was with a mass flow of 2 mg/s.

The ion-neutral mean free path for these pressures is 10 microns or less which is much less than the characteristic dimensions, so the discharge can be considered in the high pressure laminar flow regime. From the

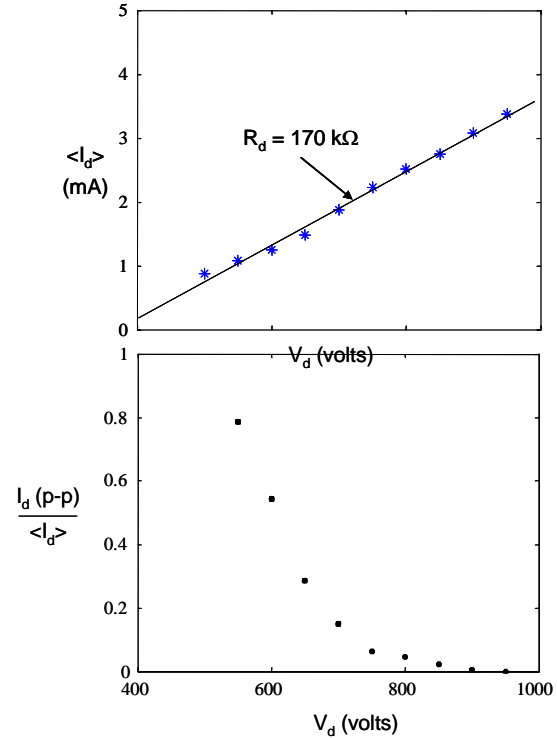


Figure 7. Current voltage characteristic of a micro-discharge. The top plot is the average current as a function of discharge voltage for a micro-discharge configuration as depicted in Fig. 1. The lower plot is the peak to peak oscillatory component of the discharge normalized to the average discharge current. Argon flow rate was 2 mg/s for all data.

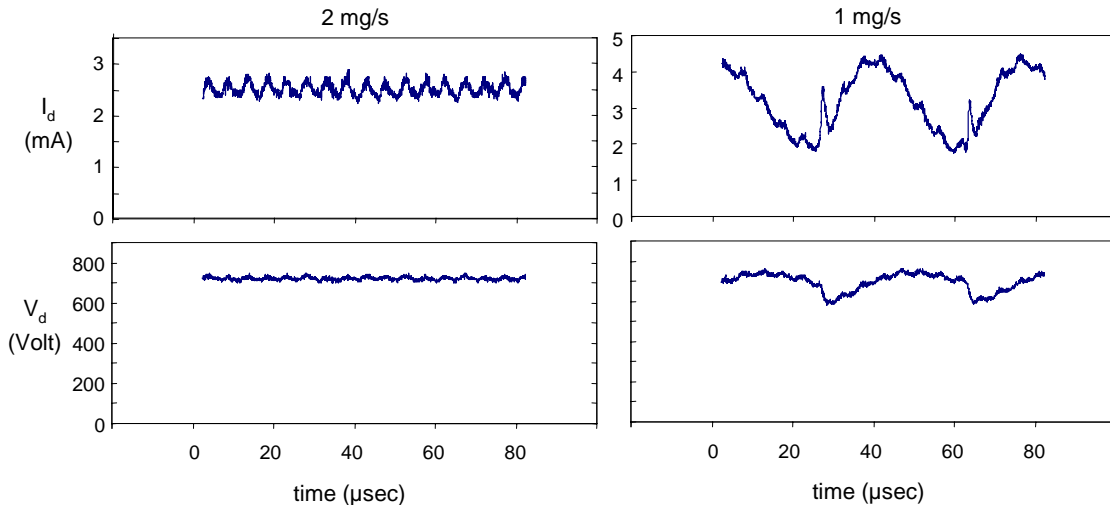


Figure 8. Time history of discharge current and voltage. The current and voltage traces were obtained by differential input probes on a floating oscilloscope for two different flow rates with the same mean discharge voltage.

conductance of the discharge channel in this regime, a mean neutral Ar channel density of $4 \times 10^{23} \text{ m}^{-3}$ is inferred. Equating the volume ionization to total surface particle loss at the Bohm velocity, it can be seen that the plasma production is primarily determined by the neutral gas density and the neutral species cross-section for ionization. There is no direct dependence on plasma density, and the effective electron temperature can be determined from the known dependence of the ionization rate on electron temperature. The inferred temperature for the microdischarge was 2 eV.

The micro-discharge operated in a regime that has characteristics of both an arc and an abnormal glow. A plot of the mean discharge current as a function of the discharge voltage is given in Fig. 7. It can be seen that the discharge voltage is large and the voltage-current characteristic is steep and positive as one would observe for an abnormal glow. The current density at the electrodes however is large (\sim several A/cm^2) due to the small electrode area. This is more in the regime of a thermionic arc. Part of the hybrid nature of the discharge is related to the small scale where the normal cathode fall thickness, $P_c d \sim 0.4 \text{ kPa-mm}$, extends well into the discharge channel for the micro-discharge geometry employed here.

The physics of the discharge is thus rather complex. The temporal behavior of the discharge reveals oscillatory behavior under all modes of operation. These oscillations are independent of whether the discharge is ballasted by an inductive or resistive impedance. In an optimum discharge, the oscillations were small and at high frequency (see Fig. 8). For lower voltage, or lower pressures, an ever large oscillatory component is observed (see Fig. 8). This corresponds to the growing dependence on the capacitive coupling to produce the discharge. All of this data was acquired with the battery powered supply so that this degree of oscillatory behavior is most likely unavoidable. It is not clear that this is a bad thing. The discharge has been sustained for many hours with large oscillations present. There is clearly evidence of cathode erosion, but it is not clear if the presence of the oscillations increases (or decreases) the rate. There is no observed erosion of the anode in any mode of operation. Only long term operation in a controlled space-like environment will settle these issues.

The power flow into the discharge indicated that very little power is lost in thermal conduction to the thruster walls. Thruster operation with a thermocouple mounted to a BN outer housing was performed to measure the heating rate of the thruster. Calculating the heat capacity of the thruster and the measured rate of heating allowed for an estimation of the thermal flow to the thruster wall. For a thruster mass of 2 g consisting of BN and Ta, and a $I_d \cdot V_d$ product of 3.6 Watts, the observed thruster heating rate reflected a heating input power of 1.0 watt. This same rate was observed over a range of thruster operation times from 5 to 60 sec, indicating that thermal flow out of the thruster to the gas feed, or radiative losses were negligible. The remaining 2.6 Watts, 72% of the total input power, was carried away by the discharge. Plasma modeling indicates a plasma density in the throat $\sim 10^{20} \text{ m}^{-3}$. Assuming an axial flow loss from the discharge channel at the sound speed for a 2 eV plasma, the ion-electron production rate of $1.6 \times 10^{16} \text{ s}^{-1}$ is inferred. With $T_e \sim 2 \text{ eV}$ there will be roughly 80 eV of radiative and ionization loss per ionization. This represents a negligible frozen flow loss of $\sim 0.2 \text{ Watt}$. The large mass particle energy is highly coupled, but the exact nature of the heating is not easily understood. Joule heating would quickly heat the electrons to very high temperature, but turbulent mixing would rapidly transfer this energy to the bulk ions and neutrals. If this is what is occurring, with approximately 2.4 W of power flowing into 1 mg/s of argon gas, the resulting kinetic velocity of the gas would be 2.2 km/s. The nozzle conversion of this energy would result in an Isp of 220 s and a thrust of 2.2 mN.

IV. Conclusions

An experimental facility has been developed to explore the possibility of employing a micro-discharge in a very simple linear structure (aperture $\sim 300 \text{ }\mu\text{m}$) as a micro-thruster. The micro-discharge provides for power addition to the neutral gas in the transition from relatively high pressure ($\sim 10 - 30 \text{ Torr}$) to vacuum through a micro-nozzle. A fairly stable discharge is maintained in a regime that produces a plasma electron temperature $\sim 2 \text{ eV}$. and deposits power into the neutral Argon gas in the range of 1 to 5 Watts. A crude measurement of the power deposition into the gas via an energy balance approach was obtained from thermocouple measurements, which also imply that the gas temperature may be as high as 1-2 eV at an efficiency that could be as high as 50 to 70%. The operation of the discharge can be strongly influenced by facility effects, particularly capacitive coupling to the vacuum chamber wall. A space relevant, battery powered, discharge supply was developed that was capable of producing a microdischarge at up to 900V and 5 mA with minimal stray coupling. This allowed for the characterization of the thruster performance under various electrode configurations. Future work will focus on the validation of these results in a large chamber. Thrust and Isp measurements, as well as longevity tests will be an integral part of future experimental work as well. In addition, experimentation and numerical simulation will be developed to better understand the physics of these small but complex discharges.

Acknowledgments

This work was sponsored by the Air Force Research Laboratory, Edwards Air Force Base.

References

- ¹R.M Myers,.S.R. Oleson,, F.M. Curren, and S.J. Schneider, "Small Satellite Propulsion Options," AIAA Paper 94-2997, June 1994.
- ²J. Mueller, "Thruster Options for Microspacecraft: A Review and Evaluation of Existing Hardware and Emerging Technologies," AIAA Paper 97-3058, July 1997.
- ³M.M. Micci, and A.D. Ketsdever. Editors, "Micropropulsion for Small Spacecraft", Progress in Astronautics and Aeronautics Vol.187, American Institute of Aeronautics and Astronautics, 2000.
- ⁴M. Martinez-Sanchez and J.E. Pollard, "Spacecraft Electric Propulsion-An Overview", Journal of Propulsion and Power, Vol.14, No.5, 1998, pp.688-699.
- ⁵J.M. Sankovic and D.T. Jacobson, "Performance of a Miniaturized Arcjet", AIAA Paper 95-2822, July 1995.
- ⁶A.D. Ketsdever, D.C. Wadsworth, P.G. Wapner, M.S. Ivanov, G.N. Markelov, "Fabrication and Predicted Performance of Conical DeLaval Micronozzles" AIAA Paper 99-2724, July 1999.
- ⁷H. Horisawa.and I. Kimura, "Studies of Very Low Power Arcjets", Chapter 6 in Micropropulsion for Small Spacecraft (M.M Micci and A.D. Ketsdever, eds.), Progress in Astronautics and Aeronautics Vol.187, pp.185-197, American Institute of Aeronautics and Astronautics, 2000.